Available online at www.sciencedirect.com

ScienceDirect

Biochimie Open 1 (2015) 28–39

www.elsevier.com/locate/biopen

Proline substitutions in a Mip-like peptidyl-prolyl *cis-trans* isomerase severely affect its structure, stability, shape and activity

Soumitra Polley[a], Devlina Chakravarty[a], Gopal Chakrabarti[b], Rajagopal Chattopadhyaya[a], Subrata Sau[a,*]

[a] *Department of Biochemistry, Bose Institute, P-1/12, CIT Scheme VII M, Kolkata 700054, West Bengal, India*
[b] *Dr. B.C. Guha Centre for Genetic Engineering, University of Calcutta, Ballygunge Circular Road, Kolkata 700019, West Bengal, India*

Received 12 May 2015; accepted 12 July 2015
Available online 23 July 2015

Abstract

FKBP22, an *Escherichia coli*-specific peptidyl-prolyl *cis-trans* isomerase, shows substantial homology with the Mip-like virulence factors. Mip-like proteins are homodimeric and possess a V-shaped conformation. Their N-terminal domains form dimers, whereas their C-terminal domains bind protein/peptide substrates and distinct inhibitors such as rapamycin and FK506. Interestingly, the two domains of the Mip-like proteins are separated by a lengthy, protease-susceptible α-helix. To delineate the structural requirement of this domain-connecting region in Mip-like proteins, we have investigated a recombinant FKBP22 (rFKBP22) and its three point mutants I65P, V72P and A82P using different probes. Each mutant harbors a Pro substitution mutation at a distinct location in the hinge region. We report that the three mutants are not only different from each other but also different from rFKBP22 in structure and activity. Unlike rFKBP22, the three mutants were unfolded by a non-two state mechanism in the presence of urea. In addition, the stabilities of the mutants, particularly I65P and V72P, differed considerably from that of rFKBP22. Conversely, the rapamycin binding affinity of no mutant was different from that of rFKBP22. Of the mutants, I65P showed the highest levels of structural/functional loss and dissociated partly in solution. Our computational study indicated a severe collapse of the V-shape in I65P due to the anomalous movement of its C-terminal domains. The α-helical nature of the domain-connecting region is, therefore, critical for the Mip-like proteins.

Keywords: Peptidyl-prolyl *cis-trans* isomerase; Helix α3; Mutation; Structure; Stability.

1. Introduction

A nascent polypeptide, synthesized by a living cell, needs to fold properly prior to performing any biological function. Two types of proteins that usually convert a linear polypeptide chain into its appropriate three-dimensional form are the chaperones and isomerases [1]. Of the isomerases, peptidyl-prolyl *cis-trans* isomerase (PPIase) catalyzes the slow isomerization of peptide bond preceding the Pro residue. PPIases, expressed by all living organisms, belong primarily to three structurally dissimilar families: cyclophilins, FK506-binding proteins (FKBPs) and parvulins. While parvulins are inhibited by juglone, cyclophilins and FKBPs are inhibited by cyclosporin A and FK506/rapamycin, respectively. Interestingly, the

Abbreviations: PPIase, peptidyl-prolyl *cis-trans* isomerase; FKBP22, a PPIase from *Escherichia coli* ; Mip, macrophage infectivity potentiator; NTD, N-terminal domain of FKBP22; CTD, C-terminal domain of FKBP22; rFKBP22, a polyhistidine-tagged FKBP22; I65P, a FKBP22/rFKBP22 variant carrying a Ile to Pro replacement at position 65 in the helix α3; V72P, a FKBP22/rFKBP22 variant with a Val to Pro substitution at position 72 in the helix α3; A82P, a FKBP22/rFKBP22 derivative harboring a Ala to Pro change at position 82 in the helix α3; TUGE, transverse urea gradient gel electrophoresis.

* Corresponding author. Tel.: +91 33 2569 3228; fax: +91 33 2355 3886.
E-mail address: subratasau@gmail.com, subratasau@yahoo.co.in (S. Sau).

http://dx.doi.org/10.1016/j.biopen.2015.07.001

complex formed between cyclosporin A or FK506/rapamycin and the cognate PPIase blocks T-cell activation by obstructing the specific signal transduction step [1,2]. Therefore, the cyclophilin and FKBP inhibitors are employed extensively in immunosuppressive therapy [1,2]. On the contrary, juglone is effective for treatment of different microbial infections and inflammatory diseases [3].

FKBP22, a PPIase (EC 5.1.2.8) originally purified from *Escherichia coli* [4], harbors 206 amino acid residues, forms dimers in solution and shares significant identity with several other PPIases including Mip (macrophage infectivity potentiator)-like PPIases [5–14]. In many pathogens, the Mip-like PPIases also act as virulence factors. The isomerase activity of *E. coli* FKBP22 and related proteins are inhibited by FK506 and rapamycin but not by juglone or cyclosporin A. Structural investigations revealed that these enzymes possess a V-like shape by assembling two monomers [13–16]. Each monomer is composed of an N-terminal domain (NTD), a C-terminal domain (CTD) and a domain-connecting flexible region. Dimerization of such enzymes occurs when the NTDs of two monomers interact [14,17]. In contrast, the CTD contains both the substrate-binding and the inhibitor-binding sites [14,18,19]. The V-shaped conformation appears crucial for its enzymatic activity, particularly with a protein substrate [20]. Further studies indicate that the CTD is comparatively less stable than the NTD or the intact isomerase [13,14]. Unfolding of a recombinant *E. coli* FKBP22 in the presence of urea and GdnCl occurs by a two-state and a three-state mechanism, respectively [14].

The domain-connecting hinges in many proteins appears to be crucial for preserving their conformation, stability and function [21–25]. The domain-connecting flexible regions in the *E. coli* FKBP22 and the orthologous proteins are largely structured with a lengthy, protease-sensitive helix designated α3 [14–18]. Helix α3 of FKBP22 is apparently formed by the amino acid residues 55–92 [14,18]. It was previously shown that shortening or enlarging α3 severely affected the structure, function and stability of FKBP22 [26]. Even the isolated domains lacking a bit of α3 became inactive or unstable [18,20]. Collectively, the presence of a helix in between the two domains of the Mip-like proteins could be critical for protecting their structural and functional integrities. To date, no systematic study has been performed to prove the necessity of a helix in between the two domains of any Mip-like PPIase, a promising drug target [27].

Proline, unlike other protein-forming amino acid residues, is a secondary amine and cannot contribute to the hydrogen bond generation. This residue, therefore, remains mostly missing within the α-helix and β-sheet as these protein structures are stabilized by hydrogen bonds. Previously, the indispensable role of α-helix in many proteins was demonstrated by introducing Pro into this structure [28–31]. To precisely determine the contribution of α3 to the structure, function and stability of the Mip-like PPIases, we generated three mutants of *E. coli* FKBP22 by replacing three non-polar amino acid residues in its α3 with the helix-destabilizing Pro residue. Our biochemical, biophysical and computational studies on the mutants indicate that the presence of a helix between the domains of FKBP22 is essential for maintaining the structure, protein folding ability, shape, and stability of this enzyme.

2. Materials and methods

2.1. Materials

Plasmid isolation kit and oligonucleotides were purchased from Genetix Biotech Asia Pvt. Ltd. Enzymes (RNase T1, Phusion DNA polymerase, *Dpn*I, *Nco*I, *Xho*I, etc.), DNA and protein markers were from Hysel India Pvt. Ltd. Rapamycin was purchased from BioVision, Ni-NTA resin from Qiagen and antibodies (anti-His and alkaline phosphatase-tagged goat anti-mouse antibody) from Santa cruz Biotechnology Inc. Acrylamide, bisacrylamide, glutaraldehyde were purchased from Merck; isopropyl β-D-1-thiogalactopyranoside (IPTG) from Fermentas; phenylmethane sulfonylfluoride (PMSF) from Sigma; urea from Sisco Research Laboratories. Plasmid pET28a and *E. coli* BL21 (DE3) were obtained as the gifts from late Dr. Pradosh Roy, Bose Institute. *E. coli* TOP10 was donated by Dr. Pradeep Parrack, Bose Institute. Plasmids, bacterial strains and oligonucleotides used in the present investigation are listed in Supplementary Tables 1 and 2

2.2. Basic DNA and protein tools

All basic molecular methods such as agarose gel electrophoresis, SDS-PAGE, staining of gels, Western blotting, plasmid DNA purification, DNA/protein estimation, polymerase chain reaction (PCR), cleavage of DNA by restriction endonuclease, sequencing of DNA inserts, and DNA transformation were performed as previously described [26,32–34].

2.3. Purification of different proteins

rFKBP22 was purified as described previously [26]. To express I65P, V72P, and A82P (all rFKBP22 variants harboring a specific Pro substitution mutation in helix α3), p1354, p1355, and p1356 DNAs were constructed, respectively, essentially by a standard procedure [35]. Primers I65P1 and I65P2 were used to create p1354. The p1355 DNA was generated using primers V72P1 and V72P2. The p1356 DNA was made using primers A82P1 and A82P2. To amplify all of the above plasmids, p1289 DNA [26] was used as the template. Strains SAU1354, SAU1355, and SAU1356 were produced by transforming plasmids p1354, p1355, and p1356 to *E. coli* BL21 (DE3), respectively. Proteins I65P, V72P, and A82P were purified from SAU1354, SAU1355, and SAU1356 respectively, as described [14]. Using the molecular masses of the monomeric forms of rFKBP22 and its variants, their molar concentrations were estimated.

2.4. Size, shape and structure of proteins

Glutaraldehyde-mediated chemical crosslinking and analytical gel filtration chromatography [14] were performed to gain

an understanding of the oligomeric status and the molecular mass/shape of the proteins in question.

To obtain clues about the structures of rFKBP22 and its three mutants, circular dichroism (CD) spectra (200–260 and 250–310 nm) and intrinsic tryptophan fluorescence spectra (λ_{em} = 300–400 nm and λ_{ex} = 295 nm) were recorded as described [14,36,37]. The amounts of secondary structures in proteins were determined by analyzing their far-UV CD spectra with CDNN software [38]. To study the solvent accessibility of tryptophan residues of the above proteins, acrylamide quenching of their tryptophan fluorescence and the Stern–Volmer constant K_{sv} were determined as stated earlier [14,39].

2.5. Function of proteins

To determine the enzymatic activity (k_{cat}/K_m) of protein (60 nM), RNase T1 (ribonuclease T1) refolding assay was performed as stated earlier [1,13,14,26].

The equilibrium dissociation constant (K_d) of rapamycin - protein interaction was determined by a standard procedure [14,26] with minor modifications. Briefly, 5 μM protein was equilibrated with 0–20 μM rapamycin in 12 steps followed by the recording of their tryptophan fluorescence spectra using a fluorescence spectrophotometer (Photon Technology International, USA, model QM-4CW) equipped with a Peltier system for temperature control.

2.6. Studies on the urea-exposed proteins

To understand the urea-induced unfolding of rFKBP22 and its mutants, 10 μM of each protein was exposed to 0–7 M urea for 16–18 h at 4 °C followed by the recording of their far-UV CD and intrinsic tryptophan fluorescence spectra as described [14]. Protein unfolding was also investigated by the transverse urea-gradient gel electrophoresis (TUGE) [14,40]. Refolding of urea-denatured proteins was investigated both by TUGE and tryptophan fluorescence spectroscopy [14,26].

2.7. Thermodynamic parameters of protein unfolding

Considering that protein unfolding in the presence of urea followed a two-state mechanism (N ↔ U), different parameters like f_u, the fraction of denatured protein molecules, ΔG^W, free energy change at 0 M urea, m, cooperativity parameter of unfolding, C_m, urea concentration at the midpoint of unfolding transition (i.e. urea concentration at which $\Delta G = 0$), and $\Delta\Delta G$, the difference of free energy change between rFKBP22 and its mutant, were determined using standard equations [41].

2.8. Computational studies, simulation and principal component analysis

The amino acid residues at positions 65, 72 and 82 in the model structure of FKBP22 [26] were separately replaced with a Pro residue using Coot [42]. To compare the above mutated structures with that of the wild-type FKBP22, molecular dynamics (MD) simulations were performed in explicit solvent at 300 K for 10 ns using the sander module of AMBER 10 [43]. The protein was solvated using TIP3 Box with the FF99SB force field parameters. Before MD simulation, the molecules were minimized using the 500 cycles of steepest descent followed by the 20,000 cycles of conjugate gradient. The system was heated to 300 K within 40 ps and equilibrated following minimization. Bonds involving hydrogen were constrained with the help of the SHAKE algorithm. The production run was performed for 10 ns using constant pressure periodic boundary conditions. A non-bonded cut-off distance of 12 Å and the integration time of 2 fs were used for all simulations. The RMSD (root mean square deviation) and the RMSF (root mean square fluctuation) values for the backbone atoms (C, Cα, O, N) of all proteins were determined by analyzing the resulting MD trajectories with ptraj module of AMBER 10.

To extract the dominant motions in the MD simulations of FKBP22 and its mutants, principal component analysis (PCA) was performed by a standard procedure [44–46] using Bio3D package of R [47]. The related figures and movies were generated using PyMol [48] and VMD [49]. Each dimeric protein was considered as a single system during the above computational analyses.

2.9. Basic statistical analysis

All results enclosed here include the means and standard deviations of at least three separate observations. Mean, standard deviation, and p values were determined as described [26]. Two results were deemed significant if the analogous p value was <0.05.

3. Results

3.1. Purification of helix α3 mutants

To determine whether the presence of α3 in between the two domains of Mip-like PPIases is required, we have generated three *E. coli* FKBP22 mutants I65P, V72P, and A82P by substituting three hydrophobic amino acid residues Ile 65, Val 72 and Ala 82 in this helix with a Pro residue (Fig. 1). As described in the *Legionella* Mip structure [15], the side chains of the selected residues in FKBP22 should neither interact with those of the domain-forming residues nor contribute to the stability of helix α3. Both Ile 65 and Ala 82 of *E. coli* FKBP22 align with either identical or other hydrophobic residues of the homologous proteins [13]. Moreover, these three residues are well separated and also located nearly ten residues away from the putative domains of FKBP22. Pro residue was introduced as it frequently disrupts the α-helices in proteins [50]. To carry out structural and functional investigation of the FKBP22 mutants, the polyhistidine-tagged forms of these mutants were purified to near homogeneity (Supplementary Fig. 1).

3.2. Shapes and sizes of the proline-inserted helix α3 mutants

Pro substitution in a protein may affect its shape, size, structure, stability and function. To determine if such a substitution

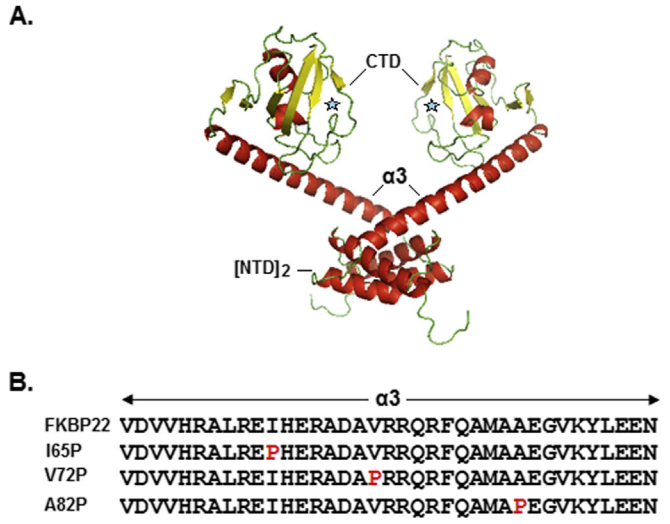

Fig. 1. Sequences and structures of proteins. (A) A tertiary model structure of *E. coli* FKBP22. The V-shaped structure of FKBP22, developed by a standard method [26], is composed of its two monomers that interact using their N-terminal domains. NTD, CTD, and α3 indicate N-terminal domain, C-terminal domain, and the domain-connecting α-helix, respectively. The asterisk denotes the putative rapamycin binding site in FKBP22. (B) Alignment of the helix α3 sequences of rFKBP22 and its Pro substitution mutants. The 'red colored' P indicates the substituted Pro residue in the helix α3 of each indicated mutant.

in α3 has altered the dimeric status of FKBP22, varying concentrations of rFKBP22, I65P, V72P, and A82P were analyzed by gel filtration chromatography individually. All of the proteins except I65P produced a single peak at both 0.5 and 20 μM (Fig. 2A). I65P resulted in a single peak at 20 μM but yielded two partly fused peaks at 0.5 μM concentration. At 20 μM, the retention volume (~74.76 mL) of V72P was nearly similar to that of rFKBP22. Their elution volumes were changed very little (~0.12 mL) upon forty fold dilution. Those of I65P and A82P were ~1.25–1.75 mL less than those of rFKBP22 or V72P at 20 μM concentration. Two peaks of I65P at 0.5 μM corresponded to the elution volumes of ~78.63 and 87.25 mL, respectively. Comparing the elution profiles of some monomeric proteins (ovalbumin, conalbumin, ribonuclease A, and carbonic anhydrase; data not shown) with those of the above proteins, we determined their apparent molecular masses. The apparent molecular mass of rFKBP22 or V72P at 0.5/20 μM is ~54.5 kDa. In contrast, the apparent masses of I65P and A82P are ~2–7 kDa higher than that of rFKBP22 or V72P at 20 μM. In addition, two partly combined peaks of I65P correspond to apparent molecular masses of ~41.42 and 22.46 kDa, respectively. Calculated molecular masses of rFKBP22, I65P, V72P and A82P monomers are nearly 23 kDa. Taken together, we suggest that rFKBP22, V72P, and A82P at 0.5/20 μM exist primarily as dimers in solution. These molecules are eluted relatively early, possibly due to their non-globular conformation in solution [13]. I65P, like rFKBP22 and other mutants, might also be dimeric in solution at 20 μM. Our chemical cross-linking data confirm that all of the rFKBP22 mutants formed dimers in solution at higher concentrations (Fig. 2B).

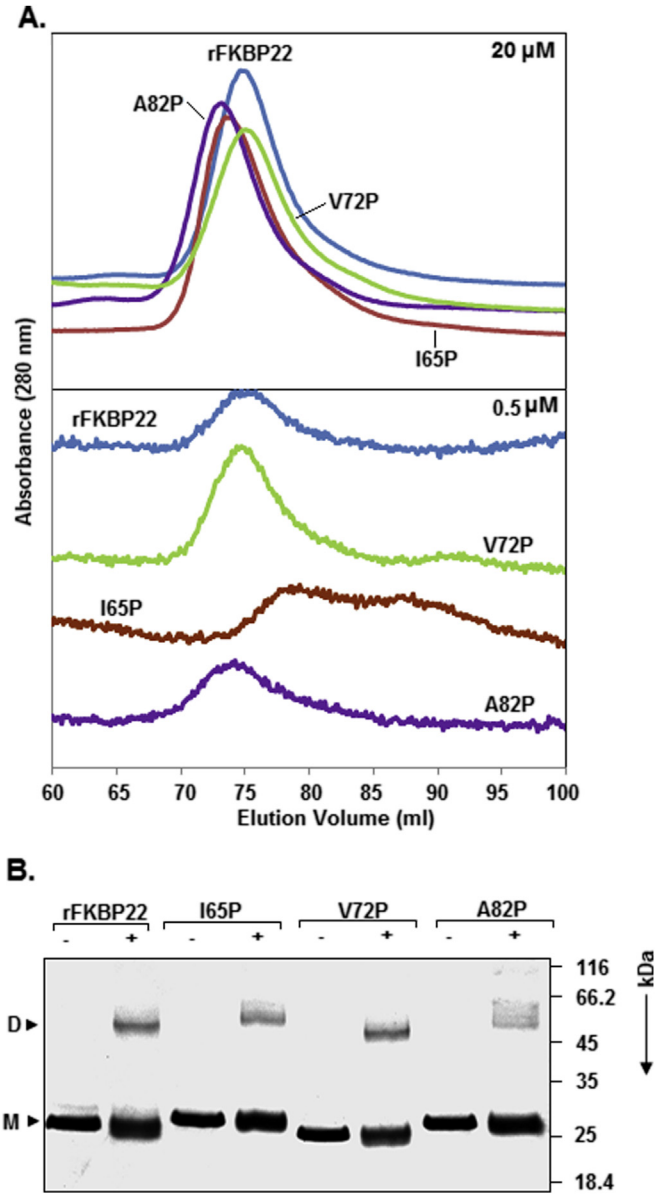

Fig. 2. Determination of shape and size of rFKBP22 and its helix α3 substitution mutants. (A) Analysis of the proteins by analytical gel filtration chromatography. Elution profile of each indicated protein (20 or 0.5 μM) was generated by passing it through a Superdex S-200 column. (B) Analysis of the glutaraldehyde-exposed (+) and unexposed (−) proteins as labeled, by SDS-13.5% PAGE. D and M indicate dimer and monomer, respectively.

The formation of two conjoint peaks by the dimeric I65P at 0.5 μM might be due to its partial dissociation (to monomer) at this concentration. At 20 μM, relatively early elution of dimeric I65P and A82P indicates that these molecules possess larger size compared to rFKBP22 and/or V72P. Thus introduction of I65P and A82P mutations into α3 affect both the shape and size of FKBP22 significantly.

3.3. Structures of the proline containing helix α3 mutants

To further determine the effect of these point mutations, the structures of rFKBP22 and its mutant variants were studied by both CD and intrinsic tryptophan fluorescence spectroscopy.

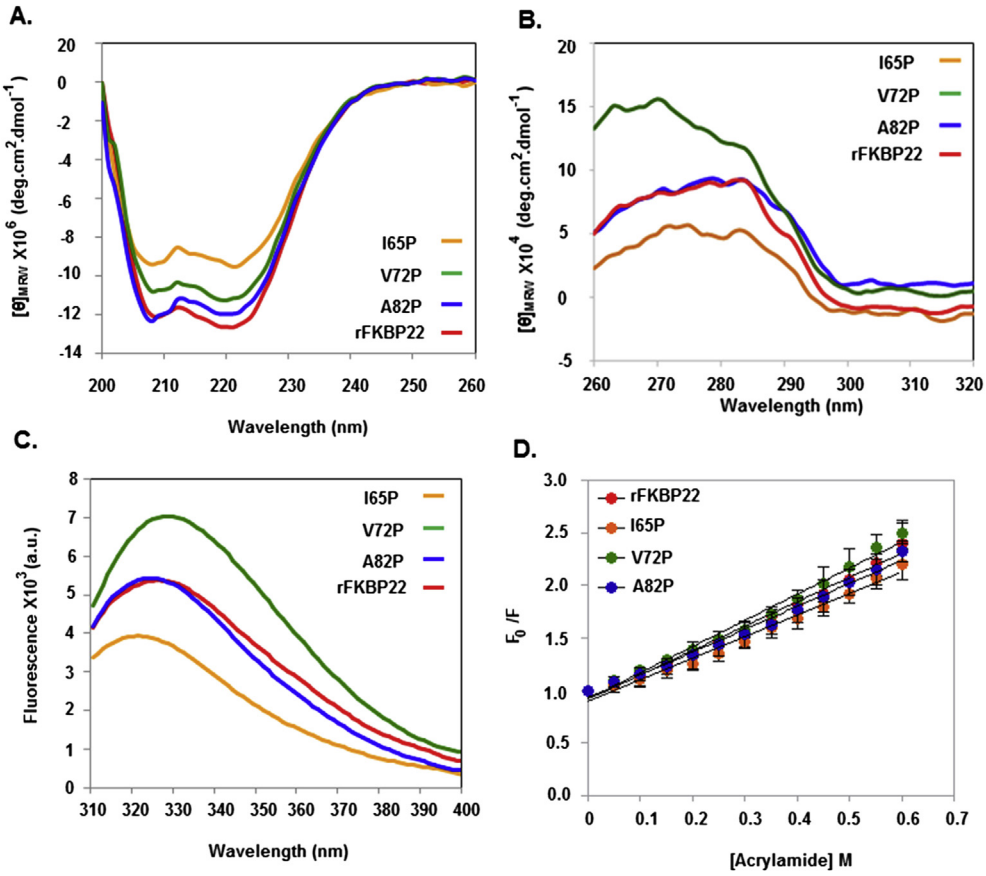

Fig. 3. Far-UV CD (A), near-UV CD (B) and intrinsic Trp fluorescence (C) spectra of rFKBP22 and its variants. (D) Stern–Volmer plots show acrylamide-mediated quenching of Trp fluorescence of rFKBP22 and its derivatives.

Fig. 3A shows the far-UV CD spectrum of each protein at 200–260 nm. Spectra of the proteins did not overlap though all of them have two peaks of large negative ellipticity at 208 and 222 nm. This indicates that these molecules are composed of different amounts of α helices. Additional analyses of the spectra by CDNN [38] showed that rFKBP22, I65P, V72P and A82P contain 37%, 27.8%, 32.9%, and 35.4% α-helix, respectively (Supplementary Table 3). Like the far-UV CD spectra, the near-UV CD spectra of I65P and V72P were completely different from that of rFKBP22 at 260–320 nm (Fig. 3B). Near UV-CD spectrum of A82P, however, appeared to partially overlap with that of rFKBP22.

The intrinsic tryptophan fluorescence spectra of I65P and V72P also differed completely from that of rFKBP22 (Fig. 3C). Compared to the tryptophan fluorescence spectrum of rFKBP22, tryptophan fluorescence spectrum of I65P yielded a less fluorescence intensity, whereas, that of V72P produced a higher intensity. The emission λ_{max} values of the associated tryptophan fluorescence spectra of rFKBP22, I65P, V72P and A82P are 327 nm, 322 nm, 329 nm and 325 nm respectively (Fig. 3C). The spectrum of A82P partly overlaps with that of rFKBP22. The λ_{max} value of V72P was red shifted compared to rFKBP22 indicating that its Trp residues may be more exposed. In contrast, Trp residues of I65P and A82P are relatively buried as the λ_{max} value of these proteins were blue shifted. Collectively, substitution of the hydrophobic amino acid residues with a Pro residue in the helix α3 affects both the secondary and the tertiary structures of FKBP22 drastically.

Stern–Volmer plots [14] produced from the acrylamide quenching data in rFKBP22 and its mutants are primarily linear (Fig. 3D). The Stern–Volmer constant K_{sv} values, calculated from the slopes of the above plots, vary from 2.04 ± 0.08 to 2.49 ± 0.09 M^{-1} (Table 1), suggesting that the environments of Trp residues in the mutants were not significantly different (in comparison with that of rFKBP22; all $p > 0.05$) though they possess altered conformations.

3.4. Activities of the proline carrying helix α3 mutants

Structural alterations as apparent from Fig. 3 may lead to changes in the drug binding affinity and/or the PPIase activity of the mutants. To determine if the drug binding affinities of FKBP22 and its mutants are different, tryptophan fluorescence quenching of these proteins was studied in the presence of 0–20 μM rapamycin (Fig. 4A). The K_d values for the rapamycin-protein interactions (Table 1) do not vary notably, indicating that substitution of the non-polar amino acid residues with a Pro in α3 did not affect the rapamycin binding affinity of FKBP22.

To determine the PPIase activities of rFKBP22 and its mutants, an RNase T1 refolding assay was performed in the

Table 1
K_{sv}, K_{cat}/K_m, and the K_d values.

Proteins	K_{sv} (M^{-1})[a]	K_d (μM)[b]	k_{cat}/K_m (μM^{-1} s^{-1})[c]
rFKBP22	2.32 ± 0.07	5.43 ± 0.57	0.818 ± 0.096
I65P	2.04 ± 0.08	5.06 ± 0.38	0.046 ± 0.010
V72P	2.49 ± 0.09	5.51 ± 0.26	0.491 ± 0.005
A82P	2.18 ± 0.07	5.41 ± 0.31	0.338 ± 0.026

[a] Stern–Volmer constants (K_{sv}) were obtained from the slopes of the plots in Fig. 3D.
[b] K_d values were estimated from Fig. 4A.
[c] k_{cat}/K_m values were calculated from Fig. 4B.

presence and absence of these proteins independently. Fig. 4B shows that enzymatic activities of mutants differ from that of rFKBP22. The k_{cat}/K_m (enzymatic activity) values for all proteins were determined (from Fig. 4B) and presented in Table 1. All of the mutants possess less PPIase activity than rFKBP22. The loss of catalytic activity was also different among the different mutants. While the loss of PPIase activity in I65P was about 94%, those in V72P, and A82P were ~40% and ~59%, respectively. As the enzymatic activities of the mutants were significantly less than that of rFKBP22 (all $p < 0.05$), we suggest that the replacement of hydrophobic amino acid residues with a Pro residue in α3 severely affected the catalytic activity of rFKBP22.

3.5. Urea-induced unfolding of proline carrying helix α3 mutants

To compare the unfolding mechanism of the α3 mutants with that of rFKBP22 [26], we recorded their far-UV CD and intrinsic tryptophan fluorescence spectra in the presence of 0–7 M urea (Supplementary Fig. S2). The unfolding curves produced using the CD data of the proteins at 222 nm are given

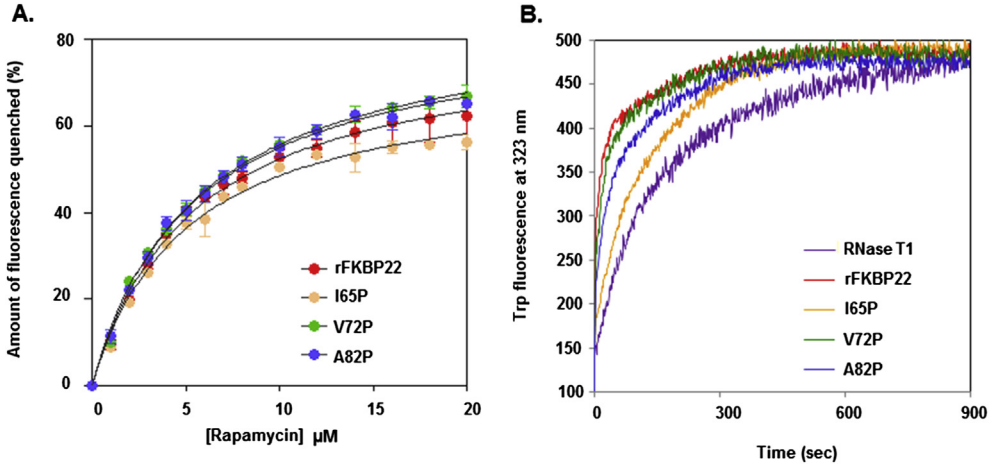

Fig. 4. Rapamycin binding and RNase T1 refolding activities of rFKBP22 and its mutants. (A) Plots show the quenching of Trp fluorescence intensity of the indicated proteins (each 5 μM) in the presence of varying concentrations of rapamycin. (B) Plots exhibit the increase of Trp fluorescence during refolding of denatured RNase T1 in the presence/absence of the indicated proteins at 10 °C.

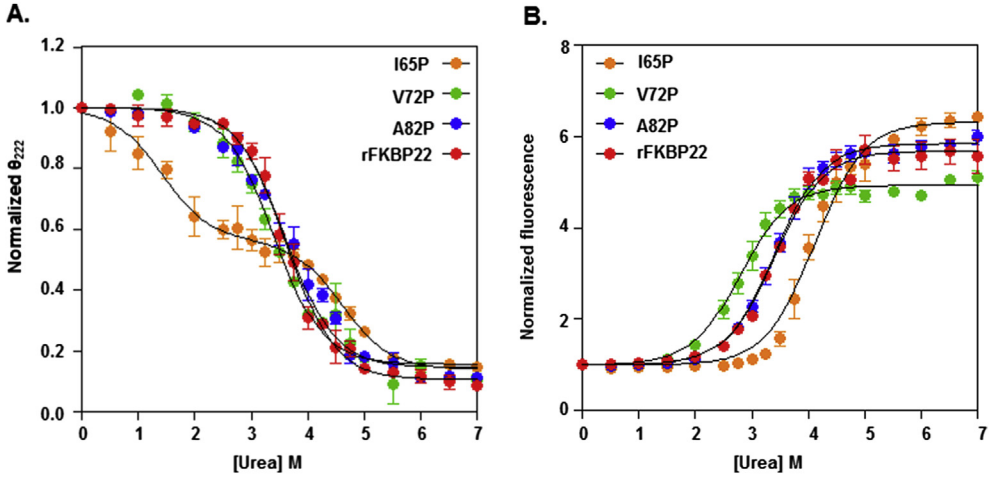

Fig. 5. Urea-induced unfolding of rFKBP22 and its mutants. (A) The plots describe the change of θ_{222} (ellipticity at 222 nm) values of the indicated proteins at 0–7 M urea. The θ_{222} values, derived from the CD spectra of the proteins (Fig. S2), were normalized as described [14]. (B) Plots show the change of the Trp fluorescence intensity values (at 326 nm) of the indicated proteins at 0–7 M urea. The Trp intensity values, obtained from the Trp fluorescence spectra of the proteins (Fig. S2), were normalized as described above. All lines through the spectroscopic signals indicate the best-fit curves.

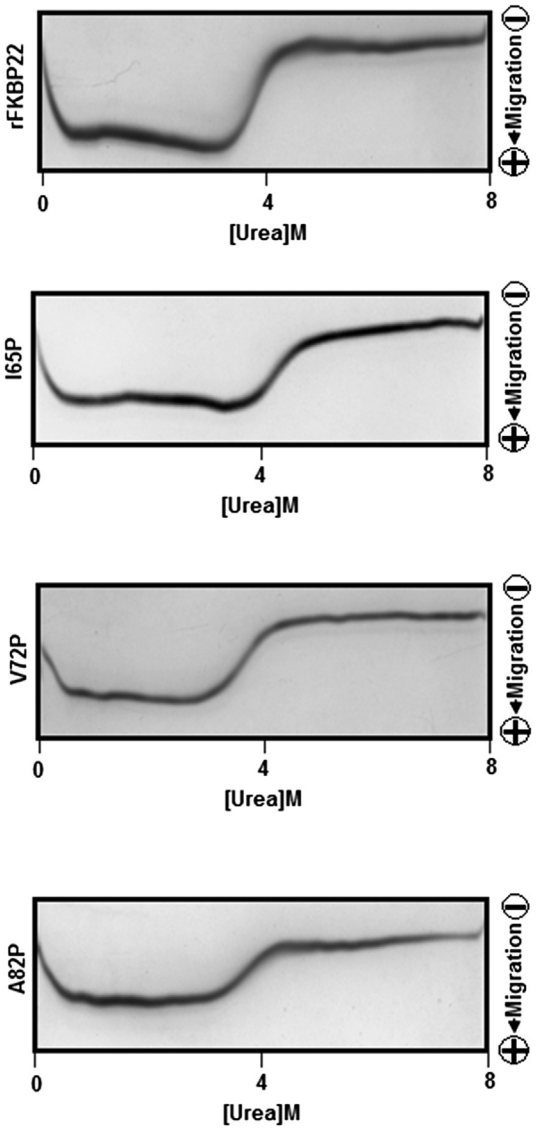

Fig. 6. Migration of rFKBP22 and its derivatives across the transverse urea gradient polyacrylamide gel.

in Fig. 5A. I65P shows a biphasic curve, whereas the rest are monophasic (Fig. 5A). Conversely, all the tryptophan fluorescence intensity curves are monophasic in nature at 0–7 M urea (Fig. 5B). Upon raising the urea concentration, λ_{max} values and intensity are both found to increase for tryptophan fluorescence, λ_{max} going to ~350 nm at the fluorescence intensity maximum (Supplementary Fig. S2). Interestingly, the curves for A82P and rFKBP22, generated by using either the Trp fluorescence or the CD data, partly overlap with the rFKBP22-specific curve, particularly, at the transition region. Further analyses by TUGE show that migration of rFKBP22 [26] and its mutants across the 0–8 M urea gradient produce nearly the sigmoidal curve-shaped bands (Fig. 6). Both spectroscopic and TUGE data indicate that the urea concentrations needed to initiate and terminate the unfolding of I65P and V72P are different from those of either rFKBP22 or A82P.

Table 2
Thermodynamic parameters from the urea-induced unfolding curves.[a]

Protein	C_m (M)	M (kcal mol^{-1} M^{-1})	ΔG^W (kcal mol^{-1})	$\Delta\Delta G$ (kcal mol^{-1})
rFKBP22	3.50 ± 0.06	1.83 ± 0.06	6.39 ± 0.34	
I65P	4.03 ± 0.06	2.47 ± 0.09	9.95 ± 0.23	1.13 ± 0.01
V72P	2.69 ± 0.02	1.93 ± 0.02	5.19 ± 0.12	1.52 ± 0.11
A82P	3.49 ± 0.08	1.77 ± 0.02	6.19 ± 0.07	0.03 ± 0.01

[a] To determine the thermodynamic parameters, the urea-induced unfolding curves, generated from the Trp fluorescence spectroscopic data of the indicated proteins, were analyzed as described in Materials and methods.

To test the reversibility in unfolding of rFKBP22 and its mutants at 0–7 M urea, they were denatured followed by their analyses using TUGE. All the proteins, like the folded counterparts (Fig. 6), show monophasic curve-shaped bands (Supplementary Fig. 3A). In addition, tryptophan fluorescence spectra of all the refolded proteins also completely superimpose with those of the corresponding native proteins (Supplementary Fig. 3B). Taken together, we conclude that urea-induced unfolding of rFKBP22 and its mutants are reversible in nature.

Previously, alteration of the length of α3 in rFKBP22 was shown to affect the molecule's stability [26]. To determine whether the helix-breaking mutations in α3 also affect the stability of rFKBP22, values of different thermodynamic parameters, such as ΔG^W, C_m, m, and $\Delta\Delta G$, were determined by fitting the sigmoidal curves (shown in Fig. 5B) to a two-state model [41]. Table 2 shows that the values of C_m (the most trustworthy thermodynamic parameter linked to the unfolding study) for rFKBP22, I65P, V72P and A82P are 3.5 ± 0.06 M, 4.03 ± 0.06 M, 2.69 ± 0.02 M and 3.49 ± 0.08 M, respectively. The ΔG^W value of I65P, similar to its C_m value, was also significantly higher, whereas, that of V72P was considerably small in comparison with other proteins (all $p < 0.05$). The free energy change $\Delta\Delta G$ between rFKBP22 and I65P or V72P were greater than 1 kcal mol^{-1} (Table 2). However, the ΔG^W or C_m values of rFKBP22 and A82P appear close to each other. C_m values of I65P and V72P determined from TUGE (Fig. 6) also support those estimated from spectroscopic studies (data not shown). In sum, the results suggest that V72P is the least stable and I65P is the most stable of the four proteins to urea denaturation.

The unfolding curves of a protein, prepared using different spectroscopic data, will not overlap if there is synthesis of intermediates during its denaturation [51–53]. To understand whether the urea-induced unfolding of rFKBP22 and its variants occurs with the generation of intermediates, the fraction of unfolded proteins were determined (using all of the spectroscopic results) and plotted against the corresponding urea concentrations. The far-UV CD data of I65P yields a biphasic curve as expected (data not shown). In contrast, all others have sigmoidal ones (Fig. 7A). Like the I65P curves, the V72P or A82P ones also do not coincide when comparing CD and fluorescence, whereas those of rFKBP22 do [14,26]. Hence, unlike rFKBP22, in the presence of 0–7 M urea, I65P, V72P and A82P may be unfolded via the synthesis of intermediate(s). To validate the above proposition, I_{320} (the Trp fluorescence intensity at 320 nm) values of these proteins were plotted against their I_{365} (Trp fluorescence intensity

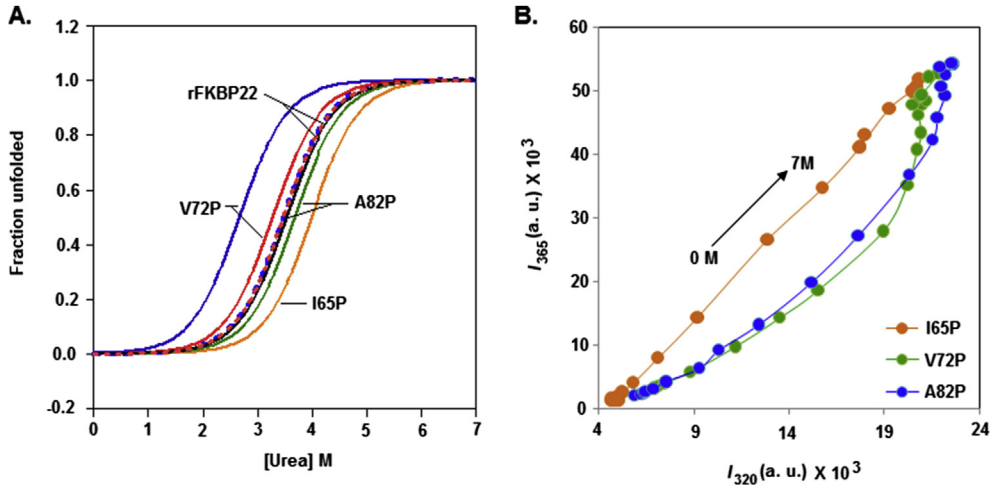

Fig. 7. Unfolding mechanism of rFKBP22 and its variants. (A) Plots of fractions of unfolded proteins versus urea concentrations. The fractions of unfolded protein molecules were determined by a standard procedure [41] using the CD and intrinsic Trp fluorescence spectra (Fig. S2) of the denoted proteins. (B) Phase diagrams show the urea-induced unfolding mechanism of I65P, V72P and A82P. I_{320} and I_{365} indicate the Trp fluorescence intensity at 320 and 365 nm, respectively.

at 365 nm) values. Such plots are usually generated to recognize the hidden unfolding/refolding intermediates of proteins [54–56]. The plots yielded by V72P and A82P diverge from the linearity at urea concentrations of above 3 M (Fig. 7B), further indicating the synthesis of intermediates during the denaturation of these mutants. Conversely, the I_{320} versus I_{365} plot (Fig. 7B) does not clearly show the synthesis of an intermediate in I65P.

3.6. Computational and statistical analyses of FKBP22 and its variants

MD simulation, a computational probe, has long been employed to understand the conformational changes in proteins with/without mutations [46,57–60]. To study the effects of α3 mutations on the conformation of FKBP22, we performed MD simulation with energy-minimized structures of both the wild-type and mutant FKBP22 proteins. Fig. 8A shows the RMSD profiles of all of the proteins during 10 ns simulation. Structures of different proteins appeared to diverge from each other roughly after 1 ns. After ~7 ns, the order of structural deviation is I65P > A82P > V72P > FKBP22. At 10 ns, the RMSD values for the wild-type, A82P, V72P and I65P are 10.7, 13.3, 10.1, 13.6 Å respectively.

The RMSF profiles also showed a similar trend with the relatively higher fluctuations in the residues of mutant structures (Fig. 8B). For reasons not clearly known, a reasonably higher flexibility was observed in the A subunit (residues 1–206) of each mutant FKBP22 protein compared to that in the B subunit (residues 207–412).

The effects of mutations on the V-shape of the FKBP22 structure were also investigated by the MD simulation probe. As expected, the V-shape of the I65P structure was severely distorted, whereas those of FKBP22, V72P and A82P were largely retained at 10 ns (Fig. 8C and Supplementary Fig. 4).

To better understand the mechanism of V-shape loss in I65P, we performed PCA using the MD simulations of FKBP22 and its mutants. In all of the proteins, the first mode corresponded to the eigenvalue of >2 Å^2 (Supplementary Movies 1–4), indicating that it would be sufficient to explain their principal motions reasonably [44]. The porcupine plots, generated with the first modes, showed the ways the motions of the mutants, particularly I65P, differed from that of the wild-type FKBP22 (Fig. 9). While the two α3-linked C-terminal domains in either FKBP22 or A82P (Fig. 9A or D) were moving in the reverse direction, those in I65P were moving towards each other (Fig. 9B). The domain movement in V72P appeared to be slightly similar to that of I65P (Fig. 9C). Taken together, the severe loss of the V-shape of I65P might be due to the abnormal movement of its domains.

Supplementary video related to this article can be found at http://dx.doi.org/10.1016/j.biopen.2015.07.001.

4. Discussion

Our studies demonstrated that the Pro substitution mutations in the helix α3 severely affected the shape, structure, protein folding ability and the unfolding mechanism of rFKBP22 (Figs. 2–7 and Table 1). Mutations (particularly at positions 65 and 72) also altered the stability of rFKBP22 notably (Table 2). In contrast, these mutants did not lose the rapamycin binding affinity though the conformations of their C-terminal domains were altered to some extent (Fig. 3C). Previously, some rFKBP22 mutants harboring a deletion or an insertion mutation in the helix α3 also exhibited similar properties [26]. Taken together, we suggest that both the presence and the length of helix α3 are crucial for preserving the structure, protein folding ability and stability of FKBP22.

Of the substitution mutants, I65P was not only associated with the highest level of structural loss (including the substantial loss of its V-shape) (Figs. 3 and 8) but also showed partial dissociation, particularly, at nanomolar concentrations (Fig. 2). Previously, an rFKBP22 mutant lacking I65 and the

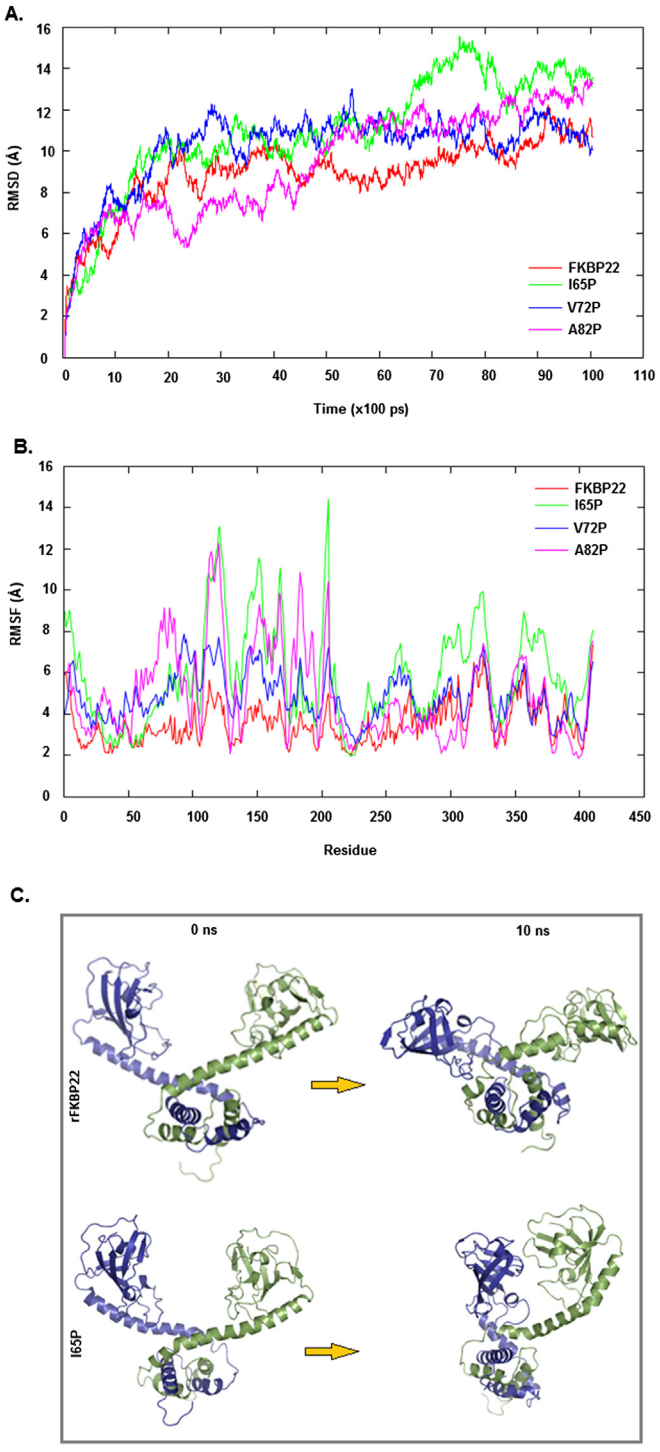

Fig. 8. MD simulation of rFKBP22 and its α3 substitution mutants. (A) RMSD profiles of the backbone atoms of the indicated proteins. (B) RMSF profiles of the amino acid residues of the denoted (dimeric) proteins. (C) Structural alteration of rFKBP22 and I65P during 10 ns MD simulation.

neighboring residues also showed partial dissociation at nanomolar concentrations and possessed an anomalous conformation [26]. In comparison with the wild-type FKBP22, this deletion mutant retained <1% PPIase activity. Various regions (such as C-terminal domain, the N-terminal domain, the V-shaped structure, and the length of helix α3) of FKBP22 and the related proteins were reported to be critical for their protein folding activity with a larger (i.e. protein) substrate [14,17–20,26,61]. The C-terminal domains of these proteins are, however, sufficient for their PPIase activity with a smaller (i.e. peptide) substrate. Although the CTD of I65P possessed an altered conformation (as evident from the Trp fluorescence spectroscopy), it retained fairly normal rapamycin binding affinity (Fig. 4A), indicating the presence of an intact catalytic center in this domain. Our quenching study (Fig. 3D) definitely supported this hypothesis as the accessibilities of two Trp residues (possibly forming the catalytic center) in the CTD of I65P were not changed notably. The CTD of I65P, therefore, may not be responsible for its decreased RNase T1 refolding ability (Fig. 4B). A previous MD simulation study indicated that a helix α3 region of *Legionella* Mip (encompassing the residues ~73–83) is one of the dynamic regions in this enzyme [62]. The dynamic nature of the above helix α3 region possibly facilitates the Mip and the related proteins to hold the bigger (protein) substrate within their V-shaped gaps [20,62]. The crystallographic *B*-values of *Legionella* Mip residues 55 to 70 (equivalent to residues 55–70 of *E. coli* FKBP22) were found higher than its mean *B*-value, indicating that the N-terminal end of helix α3 of this protein is relatively flexible in nature [15]. In I65P, destabilization of α3 due to the loss of one main chain hydrogen bond possibly made its N-terminal end more flexible, which eventually altered the V-shape of this mutant protein drastically. Taken together, we suggest that the severe loss of PPIase activity of I65P might be due to its altered V-shape and/or its partial dissociation. The conformational changes of two other substitution mutants were less drastic and hence accompanied by a moderate loss of their enzymatic activity. Collectively, the N-terminal part of helix α3 formed by residues ~55–70 contributes relatively more to keep the structure, shape, stability and function of FKBP22 intact.

Protein structures are usually stabilized by various non-covalent bonds such as hydrogen bonds, hydrophobic interactions, ionic bonds, etc. [63–65]. Several hydrogen and ionic bonds in the helix α3 were also reported to be critical for the stability of *Legionella* Mip [15]. The disruption of helix α3 by Pro substitution at positions 65, 72 and 82 had different effects on the overall conformation of FKBP22, which indicated that FKBP22 and its substitution mutants could be stabilized by a different number of non-covalent bonds. Our MD simulation study indicated that FKBP22 and its substitution mutants are composed of dissimilar numbers/extents of hydrogen bonds, ionic bonds and surface area (data not shown). All of these stabilizing factors and the structural alterations together somehow contributed to the highest or lowest stability of I65P or V72P. The reason as to why A82P and rFKBP22 are equally stable is unknown.

5. Conclusion

E. coli FKBP22 and the related proteins (including Mip-like virulence factors) are the two-domain PPIase enzymes those dimerize and adopt a V-shape through the interaction of their N-terminal domains. Using three Pro substitution mutations in the domain-connecting helix (α3) of *E. coli* FKBP22, we have

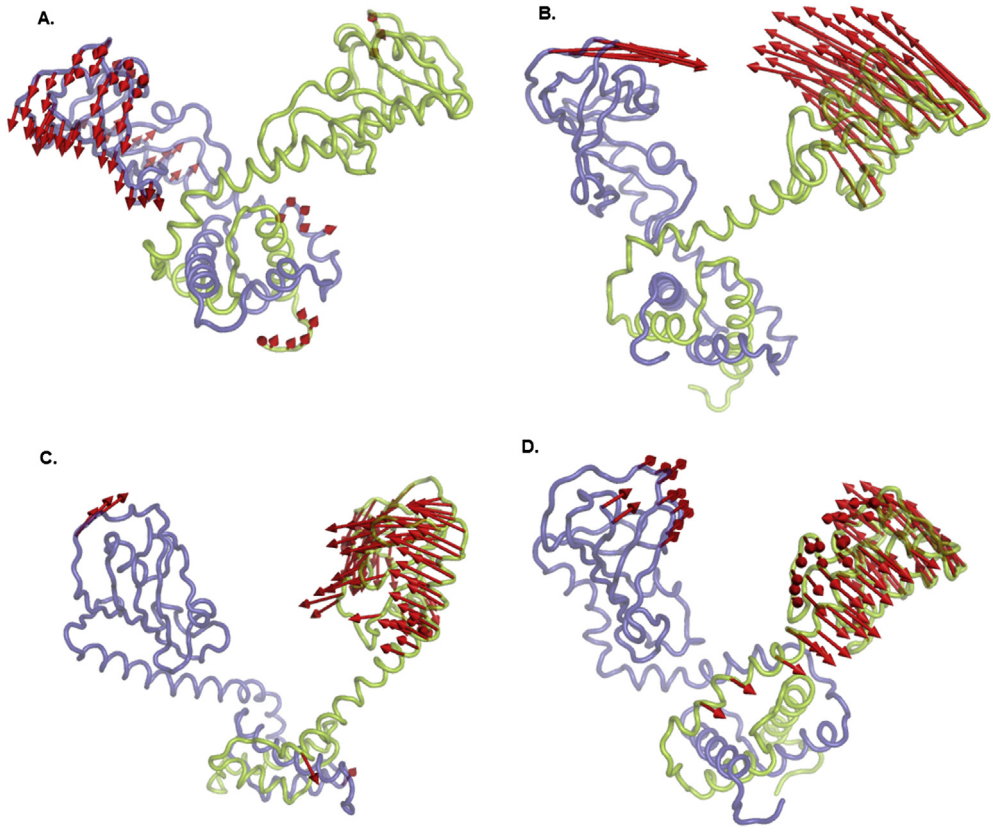

Fig. 9. Porcupine plots demonstrating dominant motions of rFKBP22 (A), I65P (B), V72P (C), and A82P (D).

demonstrated that the presence of helix $\alpha 3$ (particularly its N-terminal end) is critical for maintaining the V-shape, secondary structure, tertiary structure, dimeric status, stability, and the protein folding ability of this enzyme. The disruption of helix $\alpha 3$, however, did not alter its drug binding affinity significantly.

Conflict of interest

The authors declare no competing financial interest.

Acknowledgments

The authors thank Mr. A. Banerjee, Mr. A. Poddar, and Mr. M. Das for their excellent technical support. The authors also thank Ms C. Redfern (Wake Forest University, USA) for rectifying the manuscript. Mr. S. Polley received a Senior Research Fellowship from the Council of Scientific and Industrial Research (New Delhi, Government of India). Ms. D. Chakravarty received a Senior Research Fellowship from the Bose Institute (Kolkata, India). The work was supported by an intramural grant from Bose Institute to SS.

Appendix A. Supplementary data

Supplementary data related to this article can be found at http://dx.doi.org/10.1016/j.biopen.2015.07.001.

References

[1] S.F. Göthel, M.A. Marahiel, Peptidyl-prolyl *cis-trans* isomerases, a superfamily of ubiquitous folding catalysts, Cell. Mol. Life. Sci. 55 (1999) 423–436.

[2] C.B. Kang, Y. Hong, S. Dhe-Paganon, H.S. Yoon, FKBP family Proteins: immunophilins with versatile biological functions, Neurosignals 16 (2008) 318–325.

[3] S.C. Saling, J.F. Comar, M.S. Mito, R.M. Peralta, A. Bracht, Actions of juglone on energy metabolism in the rat liver, Toxicol. Appl. Pharmacol. 257 (2011) 319–327.

[4] J.U. Rahfeld, K.P. Rucknagel, G. Stoller, S.M. Horne, A. Schierhorn, K.D. Young, G. Fischer, Isolation and amino acid sequence of a new 22-kDa FKBP-like peptidyl-prolyl *cis/trans*-isomerase of *Escherichia coli*. Similarity to Mip-like proteins of pathogenic bacteria, J. Biol. Chem. 271 (1996) 22130–22138.

[5] N.C. Engleberg, C. Carter, D.R. Weber, N.P. Cianciotto, B.I. Eisenstein, DNA sequence of *mip*, a *Legionella pneumophila* gene associated with macrophage infectivity, Infect. Immun. 57 (1989) 1263–1270.

[6] A.G. Lundemose, J.E. Kay, J.H. Pearce, *Chlamydia trachomatis* Mip-like protein has peptidyl-prolyl *cis/trans* isomerase activity that is inhibited by FK506 and rapamycin and is implicated in initiation of chlamydial infection, Mol. Microbiol. 7 (1993) 777–783.

[7] S.M. Horne, K.D. Young, *Escherichia coli* and other species of the Enterobacteriaceae encode a protein similar to the family of Mip-like FK506-binding proteins, Arch. Microbiol. 163 (1995) 357–365.

[8] K. Ramm, A. Pluckthun, The periplasmic *Escherichia coli* peptidyl-prolyl *cis, trans*-isomerase FkpA. II. Isomerase-independent chaperone activity *in vitro*, J. Biol. Chem. 275 (2000) 17106–17113.

[9] A. Moro, F. Ruiz-Cabello, A. Fernandez-Cano, R.P. Stock, A. Gonzalez, Secretion by *Trypanosoma cruzi* of a peptidyl-prolyl *cis-trans* isomerase involved in cell infection, EMBO. J. 14 (1995) 2483–2490.

[10] R. Leuzzi, L. Serino, M. Scarselli, S. Savino, M.R. Fontana, E. Monaci, A. Taddei, G. Fischer, R. Rappuoli, M. Pizza, Ng-MIP, a surface-exposed lipoprotein of *Neisseria gonorrhoeae*, has a peptidyl-prolyl *cis/trans* isomerase (PPIase) activity and is involved in persistence in macrophages, Mol. Microbiol. 58 (2005) 669–681.
[11] N. Zang, D.J. Tang, M.L. Wei, Y.Q. He, B. Chen, J.X. Feng, J. Xu, Y.Q. Gan, B.L. Jiang, J.L. Tang, Requirement of a *mip*-like gene for virulence in the phytopathogenic bacterium *Xanthomonas campestris pv*. Campestris, Mol. Plant Microbe Interact. 20 (2007) 21–30.
[12] S.M. Horne, T.J. Kottom, L.K. Nolan, K.D. Young, Decreased intracellular survival of an *fkpA* mutant of *Salmonella typhimurium* Copenhagen, Infect. Immun. 65 (1997) 806–810.
[13] Y. Suzuki, M. Haruki, K. Takano, M. Morikawa, S. Kanaya, Possible involvement of an FKBP family member protein from a psychrotrophic bacterium *Shewanella sp.* SIB1 in cold-adaptation, Eur. J. Biochem. 271 (2004) 1372–1381.
[14] B. Jana, A. Bandhu, R. Mondal, A. Biswas, K. Sau, S. Sau, Domain structure and denaturation of a dimeric Mip-like peptidyl-prolyl *cis-trans* isomerase from *Escherichia coli*, Biochemistry 51 (2012) 1223–1237.
[15] A. Riboldi-Tunnicliffe, B. Konig, S. Jessen, M.S. Weiss, J. Rahfeld, J. Hacker, G. Fischer, R. Hilgenfeld, Crystal structure of Mip, a prolylisomerase from *Legionella pneumophila*, Nat. Struct. Biol. 8 (2001) 779–783.
[16] F.A. Saul, J.P. Arie, B. Vulliez-le Normand, R. Kahn, J.M. Betton, G.A. Bentley, Structural and functional studies of FkpA from *Escherichia coli*, a *cis/trans* peptidyl-prolyl isomerase with chaperone activity, J. Mol. Biol. 335 (2004) 595–608.
[17] Y. Suzuki, K. Takano, S. Kanaya, Stabilities and activities of the N- and C-domains of FKBP22 from a psychrotrophic bacterium overproduced in *Escherichia coli*, FEBS J. 272 (2005) 632–642.
[18] R. Köhler, J. Fanghanel, B. Konig, E. Luneberg, M. Frosch, J.U. Rahfeld, R. Hilgenfeld, G. Fischer, J. Hacker, M. Steinert, Biochemical and functional analyses of the Mip protein: influence of the N-terminal half and of peptidylprolyl isomerase activity on the virulence of *Legionella pneumophila*, Infect. Immun. 71 (2003) 4389–4397.
[19] A. Ceymann, M. Horstmann, P. Ehses, K. Schweimer, A. Paschke, M. Michael Steinert, C. Faber, Solution structure of the *Legionella pneumophila* Mip-rapamycin complex, BMC Struct. Biol. 8 (2008) 17.
[20] C. Budiman, K. Bando, C. Angkawidjaja, Y. Koga, K. Takano, S. Kanaya, Engineering of monomeric FK506-binding protein 22 with peptidyl prolyl *cis-trans* isomerase. Importance of a V-shaped dimeric structure for binding to protein substrate, FEBS J. 276 (2009) 4091–4101.
[21] M.T. Mas, Z.E. Resplandor, A.D. Riggs, Site-directed mutagenesis of glutamate-190 in the hinge region of yeast 3-phosphoglycerate kinase: implications for the mechanism of domain movement, Biochemistry 26 (1987) 5369–5377.
[22] A.V. Oleinikov, B. Perroud, B. Wang, R.R. Traut, Structural and functional domains of *Escherichia coli* ribosomal protein L7/L12. The hinge region is required for activity, J. Biol. Chem. 268 (1993) 917–922.
[23] P. Osenkowski, S.O. Meroueh, D. Pavel, S. Mobashery, R. Fridman, Mutational and structural analyses of the hinge region of membrane type 1-matrix metalloproteinase and enzyme processing, J. Biol. Chem. 280 (2005) 26160–26168.
[24] S. Dey, Z. Hu, X.L. Xu, J.C. Sacchettini, G.A. Grant, The effect of hinge mutations on effector binding and domain rotation in *Escherichia coli* D-3-phosphoglycerate dehydrogenase, J. Biol. Chem. 282 (2007) 18418–18426.
[25] B. Hou, F. Li, X. Yang, G. Hong, The properties of NodD were affected by mere variation in length within its hinge region, Acta Biochim. Biophys. Sin. Shanghai 41 (2009) 963–971.
[26] B. Jana, S. Sau, The helix located between the two domains of a mip-like peptidyl-prolyl *cis-trans* isomerase is crucial for its structure, stability, and protein folding ability, Biochemistry 51 (2012) 7930–7939.
[27] C.M. Ünal, M. Steinert, Microbial peptidyl-prolyl *cis/trans* isomerases (PPIases): virulence factors and potential alternative drug targets, Microbiol. Mol. Biol. Rev. 78 (2014) 544–571.
[28] J. Sievers, J. Errington, Analysis of the essential cell division gene ftsL of *Bacillus subtilis* by mutagenesis and heterologous complementation, J. Bacteriol. 182 (2000) 5572–5579.
[29] R.D. Gray, J.O. Trent, Contribution of a single-turn alpha-helix to the conformational stability and activity of the alkaline proteinase inhibitor of *Pseudomonas aeruginosa*, Biochemistry 44 (2005) 2469–2477.
[30] J. Feierler, M. Wirth, B. Welte, S. Schüssler, M. Jochum, A. Faussner, Helix 8 plays a crucial role in bradykinin B(2) receptor trafficking and signaling, J. Biol. Chem. 286 (2011) 43282–43293.
[31] K. Görner, E. Holtorf, J. Waak, T.T. Pham, D.M. Vogt-Weisenhorn, W. Wurst, C. Haass, P.J. Kahle, Structural determinants of the C-terminal helix-kink-helix motif essential for protein stability and survival promoting activity of DJ-1, J. Biol. Chem. 282 (2007) 13680–13691.
[32] J. Sambrook, D.W. Russell, Molecular Cloning: a Laboratory Manual, Cold Spring Harbor Laboratory Press, New York, 2001.
[33] F.M. Ausubel, Current Protocols in Molecular Biology, Greene Pub. Associates and Wiley-Interscience: J. Wiley, New York, 1987.
[34] M.M. Bradford, A rapid and sensitive method for the quantitation of microgram quantities of protein utilizing the principle of protein-dye binding, Anal. Biochem. 72 (1976) 248–254.
[35] H. Liu, J.H. Naismith, An efficient one-step site-directed deletion, insertion, single and multiple-site plasmid mutagenesis protocol, BMC Biotechnol. 8 (2008) 91.
[36] T.E. Creighton, Protein Structure: a Practical Approach, IRL Press at Oxford University Press, New York, 1997.
[37] J.R. Lakowicz, Principles of Fluorescence Spectroscopy, Kluwer Academic/Plenum, New York, 1999.
[38] G. Bohm, R. Muhr, R. Jaenicke, Quantitative analysis of protein far UV circular dichroism spectra by neural networks, Protein Eng. 5 (1992) 191–195.
[39] M.R. Eftink, C.A. Ghiron, Fluorescence quenching studies with proteins, Anal. Biochem. 114 (1981) 199–227.
[40] D.P. Goldenberg, T.E. Creighton, Gel electrophoresis in studies of protein conformation and folding, Anal. Biochem. 138 (1984) 1–18.
[41] C.N. Pace, K.L. Shaw, Linear extrapolation method of analyzing solvent denaturation curves, Proteins Suppl. 4 (2000) 1–7.
[42] P. Emsley, B. Lohkamp, W.G. Scott, K. Cowtan, Features and development of Coot, Acta Crystallogr. Sect. D. Biol. Crystallogr. 66 (2010) 486–501.
[43] D.A. Case, T.E. Cheatham, T. Darden, H. Gohlke, R. Luo, K.M. Merz, A. Onufriev, C. Simmerling, B. Wang, R.J. Woods, The Amber biomolecular simulation programs, J. Comput. Chem. 26 (2005) 1668–1688.
[44] A. Amadei, A.B. Linssen, H.J. Berendsen, Essential dynamics of proteins, Proteins 17 (1993) 412–425.
[45] M. Kurylowicz, C.H. Yu, R. Pomès, Systematic study of anharmonic features in a principal component analysis of gramicidin A, Biophys. J. 98 (2010) 386–395.
[46] P.S. Srikumar, K. Rohini, Exploring the structural insights on human laforin mutation K87A in Lafora disease – a molecular dynamics study, Appl. Biochem. Biotechnol. 171 (2013) 874–882.
[47] B.J. Grant, A.P. Rodrigues, K.M. ElSawy, J.A. McCammon, L.S. Caves, Bio3D: an R package for the comparative analysis of protein structures, Bioinformatics 22 (2006) 2695–2696.
[48] W.L. DeLano, The PyMOL Molecular Graphics System, Version 1.3r1, Schrodinger, LLC, New York, 2010.
[49] W. Humphrey, A. Dalke, K. Schulten, VMD: visual molecular dynamics, J. Mol. Graph 14 (1996) 33–38 27–8.
[50] M.S. Sansom, H. Weinstein, Hinges, swivels and switches: the role of prolines in signalling via transmembrane alpha-helices, Trends Pharmacol. Sci. 21 (2000) 445–451.
[51] T. Chatterjee, A. Pal, D. Chakravarty, S. Dey, R.P. Saha, P. Chakrabarti, Protein l-isoaspartyl-O-methyltransferase of *Vibrio cholerae*: interaction with cofactors and effect of osmolytes on unfolding, Biochimie 95 (2013) 912–921.
[52] A.N. Naganathan, U. Doshi, V. Muñoz, Protein folding kinetics: barrier effects in chemical and thermal denaturation experiments, J. Am. Chem. Soc. 129 (2007) 5673–5682.

[53] M. Oliveberg, Y.J. Tan, A.R. Fersht, Negative activation enthalpies in the kinetics of protein folding, Proc. Natl. Acad. Sci. U.S.A. 92 (1995) 8926–8929.

[54] I.M. Kuznetsova, K.K. Turoverov, V.N. Uversky, Use of the phase diagram method to analyze the protein unfolding-refolding reactions: fishing out the "invisible" intermediates, J. Proteome Res. 3 (2004) 485–494.

[55] B. Cellini, M. Bertoldi, R. Montioli, D.V. Laurents, A. Paiardini, C.B. Voltattorni, Dimerization and folding processes of *Treponema denticola* cystalysin: the role of pyridoxal 5′-phosphate, Biochemistry 45 (2006) 14140–14154.

[56] H.C. Ludwig, F.N. Pardo, J.L. Asenjo, M.A. Maureira, A.J. Yañez, J.C. Slebe, Unraveling multistate unfolding of pig kidney fructose-1,6-bisphosphatase using single tryptophan mutants, FEBS J. 274 (2007) 5337–5349.

[57] M.Z. Kamal, T.A. Mohammad, G. Krishnamoorthy, N.M. Rao, Role of active site rigidity in activity: MD simulation and fluorescence study on a lipase mutant, PLoS One 7 (2012) e35188.

[58] V. Rajendran, R. Sethumadhavan, Drug resistance mechanism of PncA in *Mycobacterium tuberculosis*, J. Biomol. Struct. Dyn. 32 (2014) 209–221.

[59] B. Kamaraj, V. Rajendran, R. Sethumadhavan, C.V. Kumar, R. Purohit, Mutational analysis of FUS gene and its structural and functional role in amyotrophic lateral sclerosis 6, J. Biomol. Struct. Dyn. 33 (2015) 834–844.

[60] S. Bhakat, A.J. Martin, M.E. Soliman, An integrated molecular dynamics, principal component analysis and residue interaction network approach reveals the impact of M184V mutation on HIV reverse transcriptase resistance to lamivudine, Mol. Biosyst. 10 (2014) 2215–2228.

[61] Y. Suzuki, O.Y. Win, Y. Koga, K. Takano, S. Kanaya, Binding analysis of a psychrotrophic FKBP22 to a folding intermediate of protein using surface plasmon resonance, FEBS Lett. 579 (2005) 5781–5784.

[62] M. Horstmann, P. Ehses, K. Schweimer, M. Steinert, T. Kamphausen, G. Fischer, J. Hacker, P. Rösch, C. Faber, Domain motions of the Mip protein from *Legionella pneumophila*, Biochemistry 45 (2006) 12303–12311.

[63] P.L. Privalov, S.J. Gill, Stability of protein structure and hydrophobic interaction, Adv. Protein Chem. 39 (1988) 191–234.

[64] C.N. Pace, B.A. Shirley, M. McNutt, K. Gajiwala, Forces contributing to the conformational stability of proteins, FASEB J. 10 (1996) 75–83.

[65] R. Jaenicke, Stability and stabilization of globular proteins in solution, J. Biotechnol. 79 (2000) 193–203.